Photoconductivity in organic thin films: From picoseconds to seconds after excitation

J. Day,[1] S. Subramanian,[2] J. E. Anthony,[2] Z. Lu,[3] R. J. Twieg,[3] and O. Ostroverkhova[1,a]

[1]*Oregon State University, Corvallis, Oregon 97331, USA*
[2]*University of Kentucky, Lexington, Kentucky 40506, USA*
[3]*Kent State University, Kent, Ohio 44242, USA*

We present a detailed study, on time scales from picoseconds to seconds, of transient and continuous wave (cw) photoconductivity in solution-grown thin films of functionalized pentacene (Pc), anthradithiophene (ADT), and dicyanomethylenedihydrofuran (DCDHF). In all films, at temperatures of 285–350 K, we observe fast carrier photogeneration and nonthermally activated charge transport on picosecond time scales. At ~ 30 ps after photoexcitation at room temperature and at applied electric field of 1.2×10^4 V/cm, values obtained for the product of mobility and photogeneration efficiency, $\mu\eta$, in ADT-tri-isoproplysilylethynyl-(TIPS)-F, Pc-TIPS, and DCDHF films are $\sim 0.018 - 0.025$, $\sim 0.01 - 0.022$, and $\sim 0.002 - 0.004$ cm^2/V s, respectively, depending on the film quality, and are weakly electric field dependent. In functionalized ADT and Pc films, the power-law decay dynamics of the transient photoconductivity is observed, on time scales of up to ~ 1 μs after photoexcitation, in the best samples. In contrast, in DCDHF amorphous glass, most of the photogenerated carriers are trapped within ~ 200 ps. Transport of photoexcited carriers on longer time scales is probed by cw illumination through an optical chopper, with a variable chopper frequency. In contrast with what is observed on picosecond time scales, charge carriers on millisecond and longer time scales are predominantly localized, and are characterized by a broad distribution of carrier lifetimes. Such carriers make the principal contributions to dc photoconductivity. © *2008 American Institute of Physics*. [DOI: 10.1063/1.2946453]

I. INTRODUCTION

Organic semiconductors have attracted attention due to their potential applications in organic thin-film transistors (TFTs), light-emitting diodes, photovoltaic cells, organic lasers, photorefractive (PR) devices, and many others.[1,2] Recently, considerable progress has been made in organic materials design and device performance:[2–7] charge carrier mobilities of over 20 cm^2/V s have been reported in rubrene and pentacene (Pc) single crystals,[8,9] power conversion efficiencies over 6% have been observed in solution-processed polymeric solar cells,[10] and PR two-beam-coupling net gain coefficients in organic glasses and polymer composites have approached 400 cm^{-1}.[2] However, an understanding of the physics of charge carrier generation and transport in organic semiconductors, which determine the (opto)electronic characteristics of these devices, is lacking, and basic questions regarding the nature of these processes remain open.[11–21]

One of the challenges encountered when probing the (opto)electronic properties of organic materials is that different charge generation, transport, and trapping mechanisms may dominate the performance under different experimental conditions. As a result, different experimental techniques could produce results that are difficult to compare and, often, hard to reconcile. For example, methods probing charge carrier dynamics on short (subnanosecond) time scales after photoexcitation (such as ultrafast time-resolved terahertz pulse spectroscopy,[15–18,22] infrared active vibrational

spectroscopy,[23,24] and Auston switch-based ultrafast photocurrent measurements[14,25,26]) often yield results different from those obtained using field-effect transistor,[8] space-charge-limiting current,[9] or continuous wave (cw) photoconductivity[27,28] measurements in similar materials. To reconcile these differences in each particular case and develop an understanding of all mechanisms involved, it is important to use a combination of several experimental techniques, for example, those that probe charge carrier dynamics on various time scales, in the same samples. An example of such combination is measurements of time-resolved and cw photoconductivity, which were previously applied in studies of photoconductive polymers,[29] organic single crystals,[14,30] and thin films.[31] This is a combination we used in our studies.

Among various kinds of organic semiconducting materials of particular technological interest are low-cost, solution-processable, and high-purity materials that can be cast into high-performance (photo)conductive thin films. This motivated the selection for our studies of small-molecular-weight novel photoconductive materials that form thin films with good coverage by solution deposition, namely, functionalized anthradithiophene (ADT), functionalized Pc, and dicyanomethylenedihydrofuran (DCDHF) derivatives. Functionalized ADT and Pc polycrystalline films have been previously explored in TFT applications,[3] and TFT mobilities of over 1 cm^2/V s have been recently reported in solution-deposited functionalized Pc thin films.[3,32] DCDHF derivatives are glass-forming molecules originally developed for PR appli-

a)Electronic mail: oksana@science.oregonstate.edu.

103, 123715-1

cations, and DCDHF-based monolithic amorphous glasses are among the best-performing organic PRs.[2,33,34] In addition, a number of functionalized ADT and DCDHF derivatives are highly fluorescent,[35–37] which broadens the range of their possible applications. For example, DCDHF derivatives have been utilized as fluorophores in single-molecule spectroscopy.[36,37]

In this article, we present a detailed study of photoexcited charge carrier dynamics, on time scales from several tens of picoseconds to many seconds after excitation, in functionalized ADT, functionalized Pc, and DCDHF thin films, together with semi-insulating GaAs as a benchmark. Using time-resolved photocurrent measurements, we observe fast charge carrier photogeneration and charge carrier mobility decreasing as the temperature increases, on picosecond time scales after photoexcitation, in all samples. Observed variations in decay dynamics and in equilibrium photoconductivity among these materials are correlated with differences in charge trapping and recombination properties. Measurements of time-resolved and cw photoconductivity in the same samples, as a function of various parameters, allow us to observe the charge carrier localization process that depends on the material.

II. EXPERIMENTAL

The molecules explored in this study are a novel high-performance fluorinated ADT derivative functionalized with tri-isoproplysilylethynyl (TIPS) side groups (ADT-TIPS-F),[3] a Pc derivative also functionalized with TIPS groups (Pc-TIPS),[3,16,17,32] and a 2,6-naphthalene functionalized with di-hexylamino donor and DCDHF acceptor[2,33,34] [Fig. 1(a)]. Pc-TIPS and ADT-TIPS-F both exhibit brick-wall-type crystal packing with significant π-overlap,[3,38] favoring high TFT mobility.[32] Both materials form polycrystalline films[17] when deposited from a solution, with the *a-b* plane in the plane of the film. Under similar conditions, DCDHF forms an amorphous glass[33] with a glass transition temperature (T_g) of 32 °C.

Glass substrates were prepared by photolithographic deposition of 100-nm-thick aluminum (Al) electrode pairs. Each pair consisted of ten interdigitated finger pairs, with 1 mm finger length, 25 μm finger width, and 25 μm gaps between the fingers of opposite electrodes. ADT-TIPS-F, Pc-TIPS polycrystalline, and amorphous DCDHF films with thicknesses of 0.5–2 μm were drop cast from toluene solution onto these substrates at ~60 °C. Up to ten samples of each kind were studied. Typical optical absorption spectra of films are shown in Fig. 1(b). GaAs samples were prepared by deposition of coplanar silver electrodes of 3 mm length (with a gap of 2 mm) on a semi-insulating GaAs wafer (University Wafer, Inc.).

For transient photoconductivity measurements, an amplified Ti:sapphire laser (800 nm, 100 fs, and 1 kHz) was used in conjunction with a frequency-doubling beta-barium borate (BBO) crystal to excite the samples. In GaAs samples, additional data were obtained with 800 nm pulses. Fluences in the 10–100 μJ/cm^2 range were used to excite organic films, while much lower values were used in measurements of
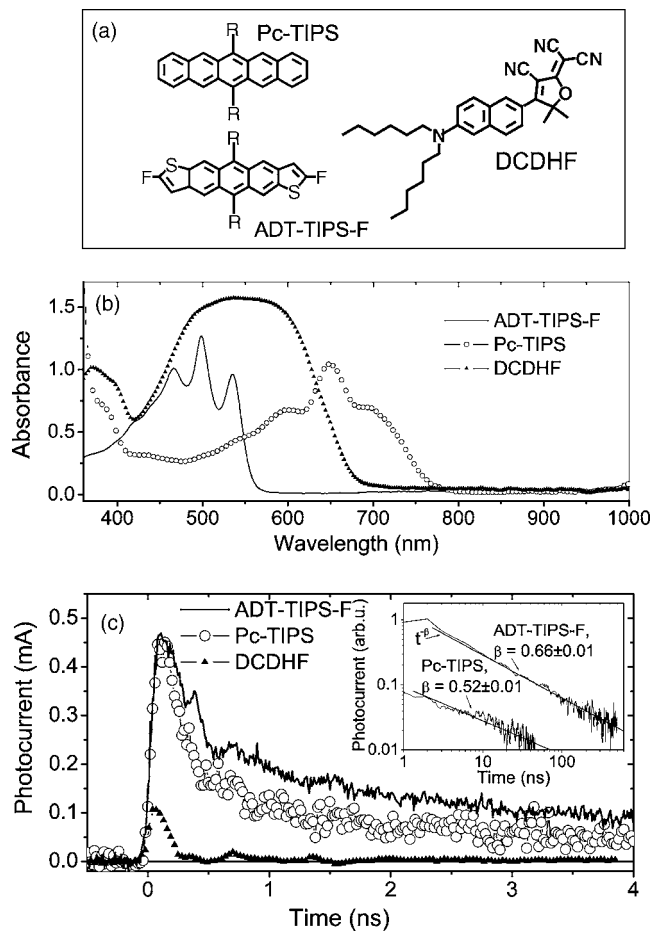
FIG. 1. (a) Molecular structures. $R=\mathrm{Si}(i\text{-Pr})_3$. (b) Optical absorption spectra of ADT-TIPS-F, Pc-TIPS, and DCDHF films. (c) Transient photocurrent obtained in ADT-TIPS-F, Pc-TIPS, and DCDHF films at 1.2×10^4 V/cm and 30 μJ/cm^2 at 400 nm. Inset: normalized transient photocurrents (I_{ph}) in ADT-TIPS-F and Pc-TIPS films. Power-law fits ($I_{ph}\propto t^{-\beta}$) are also shown. Offset along the *y* axis is for clarity.

GaAs to keep the total number density of photogenerated carriers below 10^{16} cm^{-3}. Samples were embedded in a homemade fixture, incorporating a thermoelectric unit for temperature control in the 285–350 K range; both heating and cooling cycles were used. Voltage was supplied by a Keithley 237 source-measure unit, and light pulse-induced transient photocurrent was measured with a 50 Ω load by a 50 GHz CSA8200 digital sampling oscilloscope. In the cw photoconductivity measurements, the sample was excited either by a Nd:YVO$_4$ laser at the wavelength of 532 nm or by a UV lamp and a filter combination with a center wavelength of 365 nm and a bandwidth of ~40 nm. In one set of experiments, the beam was mechanically chopped at a frequency varied between 20 and 1000 Hz, with the chopper synchronized with the reference input of a SRS830 lock-in amplifier. Photoresponse of the sample was measured as voltage across a 10 kΩ load resistor. In another set of experiments, the Keithley 237 source-measure unit was used to measure dark and cw photocurrents using the following protocol. The voltage was applied and the dark current was monitored for 5 s. Then, the light beam was opened with a shutter, illuminating the sample, and the current in the presence of light was measured over 10–20 s. The cw photocur-

rent (subsequently referred to as "dc photocurrent" or "photocurrent measured under dc conditions") was calculated as the difference between the two. In all our experiments, the samples were illuminated from the glass substrate side to minimize photoinjection and photoemission effects.[39,40] The data were taken point by point, with the samples kept in the dark between the data points to avoid accumulation of space charge.

III. RESULTS

A. Transient photoconductivity

Transient photocurrents obtained in ADT-TIPS-F, Pc-TIPS, and DCDHF films upon excitation with a 400 nm pulse at the fluence of 30 $\mu J/cm^2$ and applied electric field of 1.2×10^4 V/cm are shown in Fig. 1(c). The rise time of the transient photoresponse observed in all samples was about ~30 ps, limited by the time resolution of our setup. Following procedures detailed elsewhere,[41,42] we verified that photocurrents in Fig. 1(c) are not displacement currents, but are rather due to mobile photogenerated carriers. Data in Fig. 1(c) establish an upper limit of 30 ps for carrier photogeneration times in all materials under study, in agreement with similar studies of tetracene single crystals[14] and with optical pump-terahertz probe data for similar materials.[15–18]

Transient photocurrents observed in ADT-TIPS-F and Pc-TIPS films exhibit behavior previously observed in several organic crystals:[16–18] fast initial decay, most likely due to initial recombination and deep trapping, followed by a slow component that can be fitted with a power-law function ($I_{ph} \propto t^{-\beta}$) with $\beta \sim 0.5-0.7$ over at least three orders of magnitude [inset of Fig. 1(c)], independent of the temperature in the range studied. In agreement with previous studies,[16,17] Pc-TIPS films of different quality showed some variation in the relative contribution of the fast and slow components to decay dynamics, particularly initial decay, which reflects film-to-film deep trap density variation. In any ADT-TIPS-F sample, the initial decay was less pronounced than in the best Pc-TIPS films and even in Pc-TIPS single crystals,[43] which may imply lower deep trap density in ADT-TIPS-F. A slower initial decay at higher electric fields in ADT-TIPS-F films [Fig. 2(a)], not as pronounced in other materials, could be due to field-assisted detrapping of the carriers that became trapped in the first ~30 ps after photoexcitation. Also, in ADT-TIPS-F films, transient photocurrent [inset of Fig. 1(c)] did not completely decay up to at least the microsecond time scales, which suggests transport of mobile charge carriers even at >1 μs after photoexcitation. In contrast, in the DCDHF amorphous glass, fast decay attributed to charge trapping at deep traps was observed [Fig. 1(c)]. This prevented the observation of mobile carriers in DCDHF at times longer than approximately 200 ps after photoexcitation. In GaAs, the ultrafast photoconductivity is generally a complicated function of time.[44] However, under our experimental conditions, the decay dynamics obtained in GaAs samples could be approximated by a biexponential function. At 400 nm excitation, time constants of $\tau_1 = 0.118 \pm 0.001$ ns and $\tau_2 = 2.1 \pm 0.3$ ns were obtained. The latter time constant (τ_2) is in the range of bulk carrier lifetimes reported in the litera-
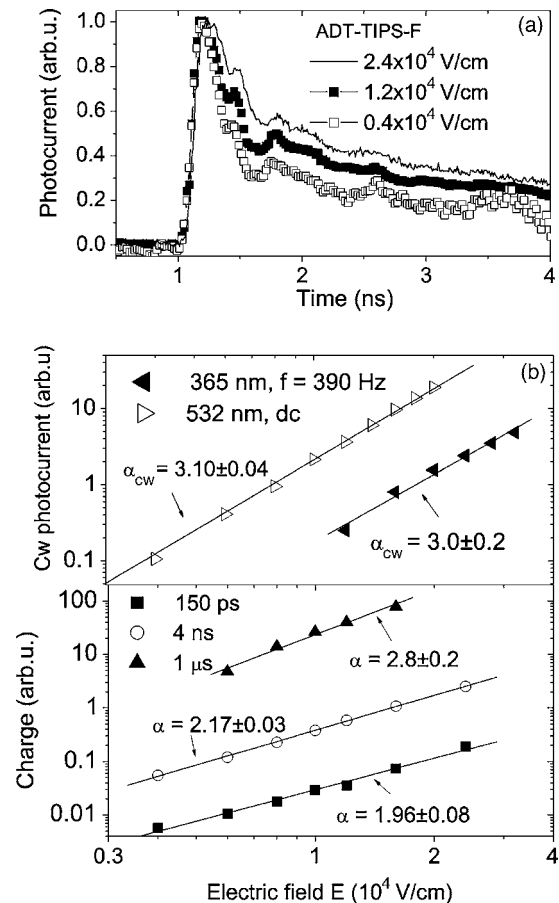
FIG. 2. (a) Normalized transient photocurrents obtained in an ADT-TIPS-F film at various electric fields. (b) Bottom: the total charge (Q) obtained by integrating the transient photocurrent with respect to time, collected over 150 ps, 4 ns, and 1 μs after photoexcitation of an ADT-TIPS-F film as a function of electric field. The power-law fits $Q \propto E^\alpha$ are also shown. Top: photocurrents (I_{cw}) obtained in the same sample under cw photoexcitation as a function of electric field. Cw photocurrents measured at 532 nm excitation under dc conditions and at 365 nm excitation at a chopper frequency (f) of 390 Hz are shown. The power-law fits $I_{cw} \propto E^{\alpha_{cw}}$ are also included.

ture for similar samples (e.g., 2.1 ns in Ref. 44 and 3.5 ns in Ref. 45). However, since at 400 nm the light penetration depth is only 14.5 nm,[46,47] τ_2 could still be affected by recombination at surface states, the process mostly likely responsible for the fast initial carrier decay characterized by a time constant of τ_1.

Electric field dependence. In all samples, the electric field dependence of the transient photocurrent amplitude could be described by a power-law function $I_{ph} \propto E^\alpha$ in the range of electric fields studied [$(0.4-4) \times 10^4$ V/cm in organic samples and $25-250$ V/cm in GaAs]. GaAs exhibited linear dependence of the transient photoresponse on the electric field (i.e., $\alpha \approx 1$). In contrast, in organic films, α varied between 1 and 1.8, depending on the sample. This is consistent with $\alpha \approx 1.6$ in tetracene single crystals recently observed in a similar experiment.[14] The electric field dependence of the shape of the transients, especially pronounced in ADT-TIPS-F films (Fig. 2), leads to a systematic change in α as a function of the time after photoexcitation. Figure 2(b) (bottom) illustrates time evolution of the electric field dependence of the collected charge (Q) obtained by integrating the

transient photocurrent with respect to time in an ADT-TIPS-F sample up to 150 ps, 4 ns, and 1 μs after photoexcitation. In this sample, α describing the field dependence of the amplitude of the transient photocurrent (data not shown) is 1.8 ± 0.1. As seen in Fig. 2(b) (bottom), α obtained from power-law fits ($Q \propto E^{\alpha}$) increases from 1.96 ± 0.08 at 150 ps to 2.8 ± 0.2 at 1 μs after photoexcitation. Also included in Fig. 2(b) (top) are electric field dependencies of the cw photocurrent (I_{cw}) in this sample measured under cw excitation at 365 nm at the chopper frequency (f) of 390 Hz and at 532 nm under dc conditions (Sec. III B). Power-law exponents α_{cw} obtained from fits with a power-law function $I_{cw} \propto E^{\alpha_{cw}}$ yield 3.0 ± 0.2 and 3.10 ± 0.04, respectively, and are higher than those observed in the transient photocurrent experiments, as discussed in Sec. IV.

The product of charge carrier mobility and photogeneration efficiency ($\mu\eta$). In all samples, the transient photocurrent was linear with respect to beam fluence, implying negligible contribution from nonlinear effects or bimolecular recombination in the range of fluences studied. From the peak values of the photocurrent, a product of the charge carrier mobility (μ) and photogeneration efficiency (η) was calculated using the relation $\mu\eta = j_0/(n_{phot}eE)$, where j_0 is the peak photocurrent density, E is the electric field, e is the electron charge, and n_{phot} is the density of absorbed photons per pulse. Generally, μ is a sum of electron and hole mobilities, but in our materials it is essentially mobility of dominant charge carriers: electrons in GaAs and holes in ADT-TIPS-F, Pc-TIPS, and DCDHF. The photogeneration efficiency η incorporates carrier loss due to trapping and recombination during the first ~30 ps after excitation not resolved in our experiment. Thus, it will be much lower than the initial efficiency, η_0, which is the number of carriers photogenerated per number of absorbed photons. This effect on $\mu\eta$ appears in values obtained for GaAs at 800 and 400 nm excitations: the value for $\mu\eta$ of ~7500 cm²/V s obtained at 800 nm at room temperature (297 K) is consistent with mobility extracted from Hall-effect measurements[46] (i.e., $\eta \approx \eta_0 = 1$) and from optical pump-terahertz probe spectroscopy,[44] while that obtained at 400 nm is much lower, ~280 cm²/V s (Fig. 3). This arises from differences in absorption coefficient at these wavelengths,[46] leading to drastically different light penetration depths (~1 μm and ~14.5 nm at 800 and 400 nm, respectively) and resulting in large contribution of a fast charge recombination at the surface at 400 nm excitation (i.e., $\eta \ll 1$ at 400 nm). At room temperature at 1.2×10^4 V/cm, the $\mu\eta$ values obtained in ADT-TIPS-F, Pc-TIPS, and DCDHF films are ~0.018–0.025, ~0.01–0.022, and ~0.002–0.004 cm²/V s, respectively, depending on the film quality.

Temperature dependence of transient photocurrent. Temperature dependence of the $\mu\eta$ values is shown in Fig. 3. In all organic samples, the $\mu\eta$ decreased as the temperature increased from 285 to 350 K, a trend qualitatively similar to that observed in GaAs (Fig. 3). A possible explanation for such behavior is that charge carrier mobility decreases as the temperature increases, which has been attributed to bandlike charge carrier transport in crystalline materials.[14–18,21,48,49] For example, a power-law dependence of charge carrier mo-
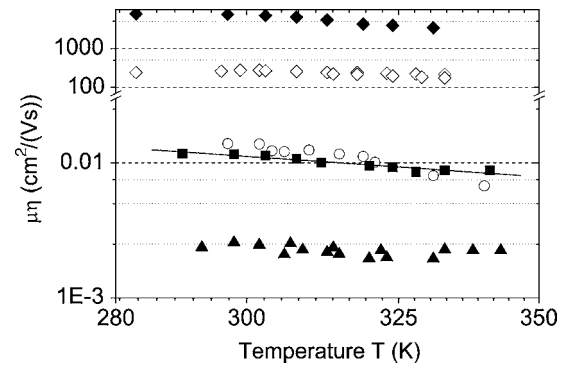
FIG. 3. Product of mobility and photogeneration efficiency ($\mu\eta$) obtained from the peak transient photocurrent in ADT-TIPS-F, Pc-TIPS, and DCDHF films (solid squares, open circles, and solid triangles, respectively) at 1.2×10^4 V/cm at 400 nm and in GaAs at 150 V/cm at 800 nm (solid diamonds) and 400 nm (open diamonds) as a function of temperature. A power-law fit ($\mu\eta \propto T^{-n}$) to the ADT-TIPS-F data, with $n = 2.3 \pm 0.2$, is also included.

bility (μ) as a function of temperature ($\mu \propto T^{-n}$) with $n = 0.5-3$ is typical of band transport[21] and has been observed in a variety of organic crystals and thin films.[9,14–18,21,48,49] The temperature dependence of the $\mu\eta$ values in ADT-TIPS-F and Pc-TIPS samples could also be fitted with the power-law function ($\mu\eta \propto T^{-n}$), with, for example, $n = 2.3 \pm 0.2$ in an ADT-TIPS-F film in Fig. 3. Interestingly, DCDHF amorphous glass, in which cw photocurrent was strongly thermally activated (Sec. III B and Ref. 34), also showed a slight decrease in $\mu\eta$ extracted from the transient photocurrent on the picosecond time scales as a function of temperature. In this case, it could be due to mobility decreasing due to increased disorder caused by a local motion of the DCDHF side groups,[34] an effect similar to that of the torsional disorder affecting subpicosecond photoconductivity in a photoconductive polymer MEH-PPV.[50] In all samples, no significant change in the transient photocurrent dynamics as a function of temperature over our range was observed.

B. cw photoconductivity

Wavelength and electric field dependence. In all organic samples studied, at the electric field of ~10^4 V/cm, even at the lowest light intensity of 0.5 mW/cm² the cw photocurrent under dc conditions was at least an order of magnitude higher than the dark current. Under 365 and 532 nm photoexcitation, the photocurrent (normalized by the number of absorbed photons) measured under similar conditions yielded similar values and exhibited similar electric field, light intensity, and chopper frequency dependencies. This suggests similar charge photogeneration mechanisms operating at these wavelengths. The electric field dependence of the cw photocurrent (I_{cw}) can be characterized by a power-law function ($I_{cw} \propto E^{\alpha_{cw}}$), with $\alpha_{cw} \approx 1$ in GaAs and α_{cw} varying between 1.8 and 3.2 in organic films, depending on the sample. Within the same sample, however, the field dependence of the cw photocurrent is stronger than that of the transient photocurrent (i.e., $\alpha_{cw} > \alpha$), as illustrated in Fig. 2(b).

Chopper frequency dependence. The dependence of the cw photocurrent (I_{cw}) on chopper frequency (f) can be de-
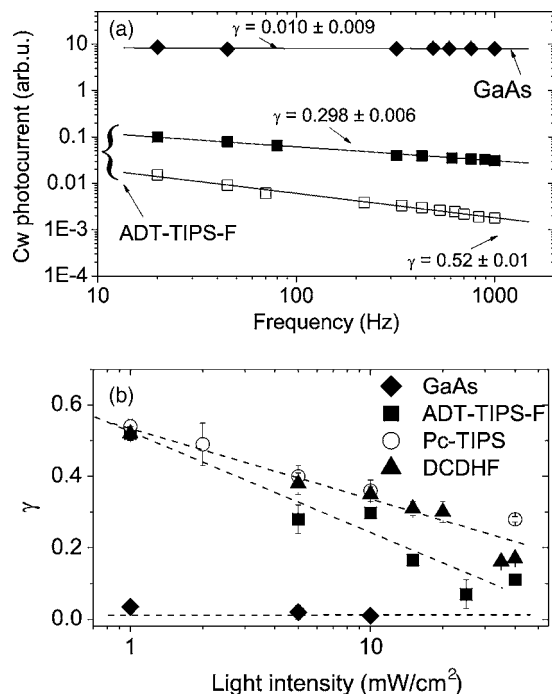
FIG. 4. (a) Cw photocurrent as a function of chopper frequency (f) obtained in the ADT-TIPS-F film at 1 mW/cm^2 (open squares) and 10 mW/cm^2 (solid squares) at 1.2×10^4 V/cm, as well as in GaAs at 1 mW/cm^2 at 150 V/cm, all at 532 nm. Power-law fits ($I_{cw} \propto f^{-\gamma}$), with exponents γ, are also shown. (b) Exponents γ as a function of light intensity obtained in ADT-TIPS-F, Pc-TIPS, and DCDHF films and GaAs. The lines are guides for the eyes.

FIG. 5. (a) Cw photocurrent as a function of light intensity (I) obtained in an ADT-TIPS-F film at 20 Hz, 390 Hz, and 1 kHz (solid, open, and crossed squares, respectively) at 1.2×10^4 V/cm, as well as in GaAs at 390 Hz and 1 kHz (solid and open diamonds, respectively) at 150 V/cm, all at 532 nm. Power-law fits ($I_{cw} \propto I^b$), with exponents b, are also shown. (b) Exponents b as a function of chopper frequency obtained in ADT-TIPS-F, Pc-TIPS, and DCDHF films and in GaAs. The lines are guides for the eyes.

scribed by a power-law function $I_{cw} \propto f^{-\gamma}$ [Fig. 4(a)]. The exponent γ decreased as light intensity (I) increased in all samples, except for GaAs, in which frequency-independent response ($\gamma \approx 0$) was observed at all intensities [Fig. 4(b)]. In organic samples, $\gamma \sim 0.5$ was observed at 1 mW/cm^2 and reached values as low as $\gamma = 0.07 \pm 0.02$ in the ADT-TIPS-F film at 25 mW/cm^2.

Light intensity dependence. The dependence of the cw photocurrent on light intensity can be described by a power-law function ($I_{cw} \propto I^b$) characterized by the exponent b varying with chopper frequency. Figure 5(a) shows the light intensity dependence of the cw photocurrent obtained in the ADT-TIPS-F film at a chopper frequency of 20 Hz, 390 Hz, and 1 kHz at 532 nm excitation. In this sample at 20 Hz, the exponent b is 0.71 ± 0.04. As the chopper frequency increases, the exponent b increases, reaching 1.02 ± 0.03 at 1 kHz, corresponding to linear dependence of the cw photocurrent on light intensity. A similar trend is observed in Pc-TIPS and DCDHF films, as illustrated in Fig. 5(b), although at low frequencies the intensity dependence in these films is closer to linear than that in the ADT-TIPS-F films. In GaAs, linear intensity dependence of the cw photocurrent, characteristic of monomolecular recombination, is observed at all frequencies (Fig. 5).

Temperature dependence. The temperature dependence of cw photoresponse obtained in ADT-TIPS-F, Pc-TIPS, and DCDHF films, as well as in the GaAs sample, at 532 nm excitation with 0.5 mW/cm^2 at a chopper frequency f of 1 kHz and under dc conditions is presented in Figs. 6(a) and 6(b), respectively. In ADT-TIPS-F films, the temperature de-

pendence of the photoresponse measured at $f = 1$ kHz showed a sample-to-sample variation, ranging between slightly negative temperature dependence (i.e., photoresponse decreasing with increasing temperature) and thermally activated response ($I_{cw} \propto \exp[-\Delta/(k_B T)]$, where k_B is the Boltzmann constant), with the activation energy Δ up to ~ 0.09 eV [Fig. 6(c) (solid squares)]. Under dc conditions, however, the same samples exhibited a thermally activated cw photocurrent, with the activation energy Δ reaching ~ 0.17 eV [Fig. 6(c) (open squares)]. Interestingly, at 1 kHz, the photoresponse in all Pc-TIPS samples studied decreased as the temperature increased [Fig. 6(a)], a behavior similar to that of the amplitude of transient photocurrent obtained on picosecond time scales (Fig. 3). Under dc conditions, however, either temperature independent or weakly thermally activated response was observed [Fig. 6(b)], with the activation energies Δ up to ~ 0.05 eV, depending on the sample. In both experiments (i.e., at 1 kHz and under dc conditions), DCDHF amorphous glass samples exhibited thermally activated behavior, with Δ of ~ 0.24–0.26 eV [Fig. 6(c)], a behavior similar to that observed in PR glasses containing previously studied DCDHF derivatives sensitized with C$_{60}$.[34] Cw photoresponse in GaAs decreased as the temperature increased [Figs. 6(a) and 6(b)], reflecting the temperature dependence of charge carrier mobility characteristic of band transport.

From dc photocurrents obtained at 532 nm excitation [Fig. 6(b)], a product of mobility (μ), initial photogeneration efficiency (η_0), and average time the carrier travels before trapping and recombination (τ) were calculated using $\mu \eta_0 \tau$
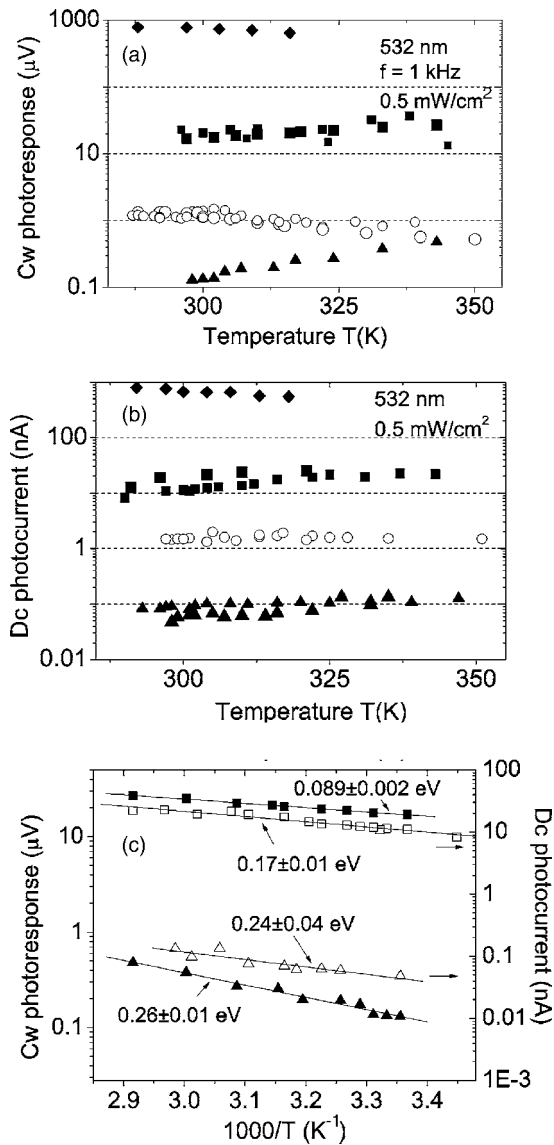
FIG. 6. Cw photocurrent as a function of temperature (T) obtained in ADT-TIPS-F, Pc-TIPS, and DCDHF films (solid squares, open circles, and solid triangles, respectively) at 0.8×10^4 V/cm and in GaAs (solid diamonds) at 100 V/cm at light intensity of 0.5 mW/cm^2 at 532 nm: (a) at a chopper frequency f of 1 kHz and (b) under dc conditions. Double and triple symbols of different sizes correspond to different samples. (c) Cw photocurrent in one of the DCDHF (triangles) and ADT-TIPS-F (squares) samples replotted as a function of 1/T: at $f=1$ kHz (solid symbols, left axis) and under dc conditions (open symbols, right axis). Arrhenius fits ($I_{cw} \propto \exp[-\Delta/(k_B T)]$), with corresponding activation energies Δ, are also shown.

$= j_{\mathrm{dc}}/(n_{\mathrm{phot}} e E)$, where j_{dc} is dc photocurrent density.[29] At room temperature at 0.8×10^4 V/cm, $\mu \eta_0 \tau$ values for ADT-TIPS-F were $\sim 6 \times 10^{-9}$ cm^2/V, similar to those observed in C$_{60}$ thin films[51] and inorganic amorphous semiconductors.[52] In Pc-TIPS and DCDHF, the corresponding values were up to one and two orders of magnitude lower, respectively (Fig. 6).

IV. DISCUSSION

Photogeneration efficiency. In all our materials, including DCDHF amorphous glass, mobile charge carriers are photogenerated on picosecond (most likely subpicosecond[16–18]) time scales [Fig. 1(b)]. From $\mu \eta$ values

of ~ 0.02 cm^2/V s, calculated from amplitudes of transient photocurrents obtained in ADT-TIPS-F and Pc-TIPS films at 1.2×10^4 V/cm, and using TFT mobility values of ~ 1 cm^2/V s in similar films,[32] we estimate a lower limit of photogeneration efficiency $\eta \sim 0.02$ at this field, similar to that obtained in tetracene single crystals in experiments utilizing Auston-switch geometry.[14] Furthermore, η is smaller than η_0 (Sec. III A). In previous studies of Pc-TIPS films using optical pump–terahertz probe time–resolved spectroscopy,[16,17] more than 90% carrier loss occurred during the first 30 ps (which is the time resolution of our transient photoconductivity setup) after photoexcitation. If a similar trend persisted under conditions of the experiments presented here, it would make the initial photogeneration efficiency η_0 in, for example, Pc-TIPS films to be at least ~ 0.2. The $\mu \eta$ value obtained from the amplitude of the transient photocurrent in DCDHF amorphous glass is rather high, reaching 0.004 cm^2/V s, which is only a factor of ~ 6 lower than in the best polycrystalline ADT-TIPS-F and Pc-TIPS films. A similar difference in $\mu \eta$ was observed on sub-picosecond time scales in amorphous and polycrystalline Pc-TIPS films,[17] which may suggest that $\mu \eta$ values similar or higher than those observed in Pc-TIPS films could be obtained in the crystalline phase of DCDHF.[33,53]

Transient decay: carrier dynamics from picoseconds to microseconds. The decay dynamics of the transient photoconductivity reflects charge trapping and recombination processes. ADT-TIPS-F and Pc-TIPS films exhibit two-component decays, with a faster component on the time scale of ~ 100 ps, most likely due to initial recombination and deep trapping, and a slower component characterized by a power-law function ($I_{\mathrm{ph}} \propto t^{-\beta}$) with $\beta \sim 0.5-0.7$ [Fig. 1(c)]. Similar power-law decay dynamics were previously observed on time scales from ~ 400 fs to at least ~ 500 ps after photoexcitation in optical pump-terahertz probe experiments in similar materials and were attributed to tunneling of nearly small molecular polarons.[16,17,54] In our experiments in ADT-TIPS-F and Pc-TIPS films, we observed similar transport evolution over time scales that extend into a microsecond range in our best films. The product of mobility and photogeneration efficiency ($\mu \eta$, obtained from the amplitude of the transient photoconductivity), decreasing as the temperature increases (Fig. 3) in ADT-TIPS-F and Pc-TIPS films (Fig. 3), would support this hypothesis. Assuming that photogeneration efficiency η does not decrease with the temperature,[55] this behavior would be attributed to the charge carrier mobility, whose resulting temperature dependence is consistent with bandlike charge transport on picosecond time scales.[15–18,21] Since decay dynamics of transient photoconductivity are temperature independent in the range studied, this suggests that the contribution of localized carriers, either lattice polarons or carriers thermally excited out of traps, to the photocurrent is not significant up to at least microseconds after photoexcitation. This is consistent with a recent demonstration that light quasiparticles, which could be nearly small molecular polarons rather than heavy lattice polarons, dominate charge transport in rubrene single crystals[13] and agree with our observation of nonthermally activated behavior of cw photoconductivity at a chopper frequency f of 1

kHz (corresponding to characteristic times of $\sim 1/(2\pi f)$ ≈ 160 μs) in Pc-TIPS and some of the ADT-TIPS-F samples. However, more studies are needed to elucidate contribution of dispersive transport, which could also be responsible for the observed power-law decay dynamics, to the transient photocurrent.

The decay dynamics of the transient photoconductivity observed in DCDHF amorphous glass indicate that most charge carriers photogenerated on picosecond time scales are trapped in deep traps within ~ 200 ps, and less than $\sim 3\%$ of the carriers contributing to the peak photocurrent are still mobile after only 3 ns. Interestingly, the amplitude of the transient photocurrent and, therefore, $\mu\eta$ values in DCDHF amorphous films are not thermally activated (Fig. 3) despite lack of crystalline order in these samples. A small decrease in $\mu\eta$ as a function of temperature could reflect an increase in disorder caused by highly temperature-dependent local motion of the DCDHF side groups, which would lower the intrinsic charge carrier mobility at higher temperatures. Such motion has been previously observed in other DCDHF derivatives, is known to occur on the microsecond time scales at $T < T_g$, and is much faster at $T > T_g$,[34] which would lower the intrinsic charge carrier mobility at higher temperatures. Apparently, large-scale molecular motion activated at around T_g in DCDHF glass, which assists in cw photoconductivity (Fig. 6 and Ref. 34) is too slow to contribute to the transient photocurrent.

Electric field dependence. In all organic samples, electric field dependence of the amplitude of the transient photoconductivity was between linear ($\alpha \approx 1$) and superlinear with $\alpha \approx 1.8$, which would suggest sublinear electric field dependence of mobility μ and photogeneration efficiency η, or both. Since at the relatively low electric fields used here (up to 4×10^4 V/cm) mobility is not likely to depend on the electric field,[56] most of this dependence would be due to η. However, our observation of an increase in α as a function of the time after photoexcitation and of α_{cw} being larger than α [e.g., in Fig. 2(b)] suggests that most of the electric field dependencies do not come from the initial photogeneration efficiency η_0, but rather from the electric-field-induced detrapping[25] of charge carriers trapped in very shallow traps within, for example, the first 30 ps after photoexcitation, or from the increasing contribution of another relatively slow process of carrier photogeneration (e.g., electric field-assisted triplet exciton dissociation) to the photocurrent at longer time scales. Although the electric-field-dependent shape of the transients, especially pronounced in ADT-TIPS-F films (Fig. 2), are more consistent with the former mechanism, detailed photophysical studies are needed to distinguish between these mechanisms and are currently in progress.

Distribution of trapping states. In all organic samples, cw photocurrent generated with 532 and 365 nm light had similar values (at the same number of absorbed photons and under the same conditions) and exhibited similar dependence on various parameters. This indicates that the same mechanism of photogeneration of mobile carriers and subsequent charge transport which contributed to cw photocurrent is operational at these wavelengths. Information about distribu-

tion of trapping states, as well as about contribution of charge carriers trapped and then released, in the cw photoconductivity, can be extracted by observing the changes in the chopper frequency dependence of the cw photocurrent as a function of light intensity and in light intensity dependence of the cw photocurrent as a function of the chopper frequency (Figs. 4 and 5, respectively). In the case of monomolecular recombination, the following chopper frequency dependence of the mobile carrier density and, therefore, photocurrent (I_{cw}) is expected: $I_{cw} \sim 1/[\sqrt{1+(\omega\tau)^2}]$, where $\omega = 2\pi f$ and τ are carrier lifetimes.[57] At $\omega\tau \ll 1$, frequency-independent photocurrent, such as that in GaAs (Fig. 4), is expected. At $\omega\tau \gg 1$, I_{cw} decreases with frequency as $1/\omega$ (i.e., $\gamma = 1$). Inclusion of bimolecular recombination yields the same behavior in these two limits.[57] Power-law frequency dependence, with $\gamma < 1$, has been observed in photoinduced absorption and photoconductivity experiments in a variety of inorganic materials and has been attributed to long-lived excitations, with stronger frequency dependence reflecting higher density of defects and impurities.[58–60] Values of $\gamma < 1$, such as those measured in our films (Fig. 4), have also been observed in semiconducting polymers (e.g., $\gamma = 0.66$ in PPV (Ref. 25) and $\gamma = 0.3$ in polydicarbazolyldiacetylene[57]) and have been attributed to a broad distribution of trapping states. At higher light intensities, the frequency dependence of the photocurrent is weaker in all samples. A similar trend was previously observed in inorganic semiconductors such as GaS crystals and explained by carrier lifetime decreasing as the intensity increases due to bimolecular recombination.[58] Qualitatively, a reduction in τ with intensity leads to an approach to the limit $\omega\tau \ll 1$ and results in an almost frequency-independent photocurrent. Among ADT-TIPS-F, Pc-TIPS, and DCDHF films, the ADT-TIPS-F films exhibited the strongest dependence of γ on light intensity, reaching γ of only ~ 0.07 at 25 mW/cm^2. This is consistent with a much higher cw photocurrent, and therefore, carrier density, in ADT-TIPS-F (Fig. 6), which leads to an enhanced bimolecular recombination.

Intensity dependence: Contribution of trapping and recombination to carrier dynamics on millisecond and longer time scales. While light intensity dependence ($I_{cw} \sim I^b$) was linear in GaAs, it was sublinear ($b < 1$) in all organic samples under dc conditions and at lower chopper frequencies, but increased to 1 at higher frequencies (Fig. 5). As sublinear intensity dependence is indicative of the presence of shallow traps ($0.5 < b < 1$) and bimolecular recombination ($b = 0.5$) in a material,[61] our results suggest that the contribution of these traps, as well as bimolecular recombination in our range of light intensities, to cw photocurrent is considerably lower at higher frequencies corresponding to time scales of several hundreds of microseconds.

Localization processes on longer time scales. Comparison between temperature dependencies of the cw photocurrent observed in ADT-TIPS-F and Pc-TIPS films at $f = 1$ kHz and under dc conditions suggests that carrier localization still proceeds on time scales from hundreds of microseconds to seconds and the contribution of localized carriers, moving by thermally activated hopping, to the cw photocurrent increases as the time progresses. In the dc limit (time

scales of tens of seconds), thermally activated cw photoconductivity is observed in most ADT-TIPS-F and Pc-TIPS samples. Larger activation energies Δ obtained in ADT-TIPS-F films compared to those in Pc-TIPS films (up to 0.17 and 0.05 eV, respectively) suggest broader distribution of trapping sites in the ADT-TIPS-F. A much higher cw photoconductivity observed in ADT-TIPS-F films compared to Pc-TIPS ones, in spite of their comparable transient photoconductivity, may indicate a much larger contribution by carriers detrapped from shallow traps into the cw photocurrent in ADT-TIPS-F. The traps are deeper in Pc-TIPS, which is consistent with the decay dynamics of the transient photoconductivity [Fig. 1(b)]. Once carriers are trapped in these deep traps, they do not contribute to the cw photocurrent measured under conditions of our experiments, but rather participate in persistent photoconductivity on the time scales of hours.[28] In DCDHF glass, complete carrier localization occurs on submillisecond time scales (most likely subnanosecond time scales as suggested by our transient photoconductivity experiments) as cw photoconductivity exhibits similar thermally activated behavior at all chopper frequencies and under dc conditions, with Δ of $\sim 0.24-0.26$ eV. GaAs is on the other end of the spectrum, with delocalized carriers contributing to transient and cw photocurrents at all time scales investigated.

V. SUMMARY

In summary, our data are consistent with the following overall picture. In ADT-TIPS-F, Pc-TIPS, and DCDHF films, mobile charge carriers are photogenerated on picosecond time scales via nonthermally activated mechanisms, assisted weakly if at all by electric fields. In ADT-TIPS-F and Pc-TIPS polycrystalline films, the charge transport mechanism at time scales from tens of picoseconds to at least several hundreds of nanoseconds is consistent with tunneling of nearly small molecular polarons. However, dispersive transport, especially at time scales longer than nanoseconds after photoexcitation, cannot be ruled out. In DCDHF amorphous glass, nonthermally activated charge transport on picosecond time scales is observed and is negatively affected by disorder caused by the local motion of the DCDHF side groups. In these films already at ~ 200 ps after photoexcitation, most charge carriers are trapped or recombined. At room temperature at 1.2×10^4 V/cm, values obtained for the product of mobility and photogeneration efficiency, $\mu\eta$, in ADT-TIPS-F, Pc-TIPS, and DCDHF films are $\sim 0.018-0.025$, $\sim 0.01-0.022$, and $\sim 0.002-0.004$ cm^2/V s, respectively, depending on the film quality.

On time scales from hundreds of microseconds to seconds after photoexcitation, an increasing contribution of localized carriers to photocurrent, together with an increasing role played by traps and, at higher light intensities, by bimolecular recombination, is observed in ADT-TIPS-F and Pc-TIPS films. At these time scales, only thermally activated hopping of localized charge carriers is observed in DCDHF glass. Although photoconductivity on picosecond time scales is similar in ADT-TIPS-F films and Pc-TIPS films, it becomes much higher on longer time scales in ADT-TIPS-F, which we associate with a larger contribution to the photocurrent in ADT-TIPS-F from carriers detrapped from shallow traps. In general, the effects of trap depth and of trapping and detrapping dynamics are more noticeable on longer time scales. The investigation of the role of trap density and trap depth, as well as exciton dynamics, in charge carrier dynamics in these materials is currently underway.

[1] S. R. Forrest, Nature (London) **428**, 911 (2004).
[2] O. Ostroverkhova and W. E. Moerner, Chem. Rev. (Washington, D.C.) **104**, 3267 (2004).
[3] J. E. Anthony, Chem. Rev. (Washington, D.C.) **106**, 5028 (2006).
[4] A. R. Murphy and J. M. J. Frechet, Chem. Rev. (Washington, D.C.) **107**, 1066 (2007).
[5] J. Zaumseil and H. Sirringhaus, Chem. Rev. (Washington, D.C.) **107**, 1296 (2007).
[6] I. D. W. Samuel and G. A. Turnbull, Chem. Rev. (Washington, D.C.) **107**, 1272 (2007).
[7] Y. Shirota and H. Kageyama, Chem. Rev. (Washington, D.C.) **107**, 953 (2007).
[8] V. Podzorov, E. Menard, A. Borissov, V. Kiryukhin, J. A. Rogers, and M. E. Gershenson, Phys. Rev. Lett. **93**, 086602 (2004).
[9] O. D. Jurchescu, J. Baas, and T. T. M. Palstra, Appl. Phys. Lett. **84**, 3061 (2004).
[10] J. Y. Kim, K. Lee, N. E. Coates, D. Moses, T. Q. Nguyen, M. Dante, and A. J. Heeger, Science **317**, 222 (2007).
[11] N. S. Sariciftci, *Primary Photoexcitations in Conjugated Polymers: Molecular Exciton Versus Semiconductor Band Model* (World Scientific, Singapore, 1997).
[12] F. A. Hegmann, Phys. Can. **59**, 127 (2003).
[13] Z. Li, V. Podzorov, N. Sai, M. C. Martin, M. E. Gershenson, M. Di Ventra, and D. N. Basov, Phys. Rev. Lett. **99**, 016403 (2007).
[14] D. Moses, C. Soci, X. Chi, and A. P. Ramirez, Phys. Rev. Lett. **97**, 067401 (2006).
[15] V. K. Thorsmølle, R. D. Averitt, X. Chi, D. J. Hilton, D. L. Smith, A. P. Ramirez, and A. J. Taylor, Appl. Phys. Lett. **84**, 891 (2004).
[16] O. Ostroverkhova, D. G. Cooke, S. Shcherbyna, R. F. R. F. Egerton, F. A. Hegmann, R. R. Tykwinski, and J. E. Anthony, Phys. Rev. B **71**, 035204 (2005).
[17] O. Ostroverkhova, S. Shcherbyna, D. G. Cooke, R. F. Egerton, F. A. Hegmann, R. R. Tykwinski, S. R. Parkin, and J. E. Anthony, J. Appl. Phys. **98**, 033701 (2005).
[18] O. Ostroverkhova, D. G. Cooke, F. A. Hegmann, J. E. Anthony, V. Podzorov, M. E. Gershenson, O. D. Jurchescu, and T. T. M. Palstra, Appl. Phys. Lett. **88**, 162101 (2006).
[19] R. Schuster, M. Knupfer, and H. Berger, Phys. Rev. Lett. **98**, 037402 (2007).
[20] H. Marciniak, M. Fiebig, S. Schiefer, B. Nickel, F. Selmaier, and S. Lochbrunner, Phys. Rev. Lett. **99**, 176402 (2007).
[21] V. Coropceanu, J. Cornil, D. A. da Silva Filho, Y. Olivier, R. Silbey, and J. L. Bredas, Chem. Rev. (Washington, D.C.) **107**, 926 (2007).
[22] F. A. Hegmann, O. Ostroverkhova, and D. G. Cooke, in *Photophysics of Molecular Materials*, edited by G. Lanzani (Wiley, Weinheim, 2006), pp. 367–428.
[23] D. Moses, A. Dogariu, and A. J. Heeger, Phys. Rev. B **61**, 9373 (2000).
[24] C. Soci, D. Moses, Q. H. Xu, and A. J. Heeger, Phys. Rev. B **72**, 245204 (2005).
[25] D. Moses, H. Okumoto, C. H. Lee, A. J. Heeger, T. Ohnishi, and T. Noguchi, Phys. Rev. B **54**, 4748 (1996).
[26] H. Y. Liang, W. L. Cao, M. Du, Y. Kim, W. N. Herman, and C. H. Lee, Chem. Phys. Lett. **419**, 292 (2006).
[27] T. Tokumoto, J. S. Brooks, R. Clinite, X. Wei, J. E. Anthony, D. L. Eaton, and S. R. Parkin, J. Appl. Phys. **92**, 5208 (2002).

[28] J. S. Brooks, T. Tokumoto, E. S. Choi, D. Graf, N. Biskup, D. L. Eaton, J. E. Anthony, and S. A. Odom, J. Appl. Phys. **96**, 3312 (2004).

[29] D. Moses, J. Wang, G. Yu, and A. J. Heeger, Phys. Rev. Lett. **80**, 2685 (1998).

[30] G. Horowitz, F. Kouki, P. Valat, P. Delannoy, and J. Roussel, Phys. Rev. B **59**, 10651 (1999).

[31] C. H. Lee, G. Yu, D. Moses, V. I. Srdanov, X. Wei, and Z. V. Vardeny, Phys. Rev. B **48**, 8506 (1993).

[32] S. K. Park, T. N. Jackson, J. E. Anthony, and D. A. Mourey, Appl. Phys. Lett. **91**, 063514 (2007).

[33] O. Ostroverkhova, U. Gubler, D. Wright, W. E. Moerner, M. He, and R. Twieg, Adv. Funct. Mater. **12**, 621 (2002).

[34] O. Ostroverkhova, W. E. Moerner, M. He, and R. Twieg, ChemPhysChem **4**, 732 (2003).

[35] A. P. Platt, J. Day, M. J. Kendrick, S. Subramanian, J. E. Anthony, and O. Ostroverkhova, *CLEO-QELS* (Optical Society of America, Baltimore, MD, 2007).

[36] K. A. Willets, O. Ostroverkhova, M. He, R. J. Twieg, and W. E. Moerner, J. Am. Chem. Soc. **125**, 1174 (2003).

[37] K. A. Willets, S. Y. Nishimura, P. J. Schuck, R. J. Twieg, and W. E. Moerner, Acc. Chem. Res. **38**, 549 (2005).

[38] O. Ostroverkhova, D. G. Cooke, F. A. Hegmann, R. R. Tykwinski, S. R. Parkin, and J. E. Anthony, Appl. Phys. Lett. **89**, 192113 (2006).

[39] D. Moses, C. Soci, P. Miranda, and A. J. Heeger, Chem. Phys. Lett. **350**, 531 (2001).

[40] C. Im, E. V. Emelianova, H. Bassler, H. Spreitzer, and H. Becker, J. Chem. Phys. **117**, 2961 (2002).

[41] E. L. Frankevich, Chem. Phys. Rep. **17**, 2069 (1999).

[42] C. H. Lee, G. Yu, D. Moses, and A. J. Heeger, Phys. Rev. B **49**, 2396 (1994).

[43] F. A. Hegmann, O. Ostroverkhova, J. Gao, L. Barker, R. R. Tykwinski, J. E. Bullock, and J. E. Anthony, Proc. SPIE **5352**, 196 (2004).

[44] M. C. Beard, G. M. Turner, and C. A. Schmuttenmaer, Phys. Rev. B **62**, 15764 (2000).

[45] P. Parkinson, J. Lloyd-Hughes, Q. Gao, H. H. Tan, C. Jagadish, M. B. Johnston, and L. M. Herz, Nano Lett. **7**, 2162 (2007).

[46] J. S. Blakemore, J. Appl. Phys. **53**, R123 (1982).

[47] O. E. Madelung, *Semiconductors Basic Data* (Springer-Verlag, Berlin, 1996).

[48] N. Karl, Synth. Met. **133–134**, 649 (2003).

[49] N. Karl, in *Organic Electronic Materials*, Springer Series in Materials Science, edited by R. Farchioni and G. Grosso (Springer, New York, 2001), p. 449.

[50] E. Hendry, J. M. Schins, L. P. Candeias, L. D. A. Siebbeles, and M. Bonn, Phys. Rev. Lett. **92**, 196601 (2004).

[51] G. Priebe, B. Pietzak, and R. Könenkamp, Appl. Phys. Lett. **71**, 2160 (1997).

[52] M. Abkowitz, A. Lakatos, and H. Scher, Phys. Rev. B **9**, 1813 (1974).

[53] O. Ostroverkhova, W. E. Moerner, M. He, and R. J. Twieg, Appl. Phys. Lett. **82**, 3602 (2003).

[54] E. A. Silinsh and V. Capec, *Organic Molecular Crystals: Interaction, Localization and Transport Phenomena* (American Institute of Physics, New York, 1994).

[55] M. Pope and C. E. Swenberg, *Electronic Processes in Organic Crystals and Polymers*, 2nd ed. (Oxford University Press, New York, 1999).

[56] J. C. Sancho-Garcia, G. Horowitz, J. L. Bredas, and J. Cornil, J. Chem. Phys. **119**, 12563 (2003).

[57] G. Dellepiane, C. Cuniberti, D. Comoretto, G. F. Musso, G. Figari, A. Piaggi, and A. Borghesi, Phys. Rev. B **48**, 7850 (1993).

[58] G. A. Gamal and M. I. Azad, Eur. Phys. J.: Appl. Phys. **32**, 1 (2005).

[59] A. Eray, G. Nobile, and F. Palma, Mater. Sci. Eng., B **102**, 398 (2003).

[60] R. Schwarz, R. Cabeca, E. Morgado, M. Niehus, O. Ambacher, C. Marques, and E. Alves, Diamond Relat. Mater. **16**, 1437 (2007).

[61] A. Rose, *Concepts in Photoconductivity and Allied Problems* (Interscience, New York, 1963).